East European Journal of Physics. 1. 9–19 (2025)
DOI: 10.26565/2312-4334-2025-1-01 ISSN 2312-4334

RECONSTRUCTION OF KANIADAKIS HOLOGRAPHIC DARK ENERGY MODEL IN SELF CREATION THEORY OF GRAVITY

Y. Aditya[a], D. Tejeswararao[a], U.Y. Divya Prasanthi[b,*], D. Ram Babu[a]
[a]Department of Basic Sciences and Humanities, GMR Institute of Technology, Rajam-532127, India
[b]Department of Statistics & Mathematics, College of Horticulture, Dr. Y.S.R. Horticultural University, Parvathipuram-535502, India
*Corresponding Author e-mail: divyaaug24@gmail.com
Received November 12, 2024; revised January 6, 2025; accepted January 25, 2025

The primary objective of this paper is to examine a Kaniadakis holographic dark energy universe of Bianchi type-II within the framework of self-creation gravity theory. In this dark energy model, the Hubble horizon is used as the infrared cutoff, following Kaniadakis' holographic dark energy concept. We calculate various dynamical parameters in this model, including the statefinder (r, s) plane, the deceleration parameter q, the equation of state (ω_{de}), the square speed of sound, and the $\omega_{de} - \omega'_{de}$ plane. A graphical analysis of these parameters is provided across a range of free parameter values. The results reveal that the deceleration parameter demonstrates the universe's smooth transition from an early decelerated phase to the current accelerated expansion, while the equation of state parameter suggests a phantom phase. The $\omega_{de} - \omega'_{de}$ plane reaches the thawing region, and the statefinder plane aligns with both the phantom model and Chaplygin gas. The current values of the parameters are consistent with existing observational data, and the strong energy conditions are found to be violated.

Keywords: *Bianchi type-II model; Kaniadakis holographic dark energy; Self creation Theory; Dark energy; Modified theory of gravity*

PACS: 98.80.-k, 95.36.+x

1. INTRODUCTION

One of the most astonishing findings in modern cosmology is that the universe is not only expanding but accelerating. Today, multiple independent observational sources support this accelerating behavior of the cosmos [1]-[3]. Explanations for this observed phenomenon fall broadly into two main approaches. In the framework of the General Theory of Relativity (GTR), the universe appears dominated by an enigmatic, negative-pressure component known as dark energy (DE), as evidenced by CMBR and LSS analyses. Alternatively, the acceleration could be explained by altering the law of gravity itself through modifications of the GTR action, known as modified gravity theories. Among these are the well-known $f(R)$ gravity [4] and Gauss-Bonnet gravity, which involves the Gauss-Bonnet invariant [5]. Other approaches include $f(R,T)$ gravity [6], as well as scalar-tensor theories like Brans-Dicke (BD) [7] and Saez-Ballester (SB) [8], along with the self-creation theory of gravitation. Barber [9] introduced two continuous creation theories: one as a variation of the BD theory and the other modifying GTR to accommodate continuous matter creation in alignment with observational data. These theories suggest a universe generated by self-contained gravitational and matter fields. Barber's second self-creation theory has inspired extensive study into diverse cosmological models (Ref. [10]-[14]). The theory provides a framework where the cosmological constant can emerge naturally from the dynamics of the gravitational field and matter. It offers a novel approach to explain cosmic acceleration and dark energy without relying on a constant energy density. Essentially, the theory proposes a self-creation of gravity, which modifies both the gravitational field equations and the evolution of the universe. For a thorough exploration of DE and modified gravity theories, please refer to the sources cited in [15]-[28].

Alternatively, some theoretical approaches attempt to resolve the DE problem by introducing novel types of matter or modified equations of state [29]-[30]. Another promising avenue is Holographic DE (HDE), rooted in the holographic principle [31, 32]. When applied to the universe, the vacuum energy associated with this principle can be interpreted as DE, or specifically HDE, as proposed by Cohen et al. [33]. Over recent decades, various entropy formulations have been applied to develop and examine cosmological models. This has led to several innovative HDE models, such as the Tsallis HDE [34, 35], Sharma-Mittal HDE (SMHDE) [36], and Renyi HDE model [37]. Numerous researchers have evaluated cosmological models based on these new HDE concepts [38]- [42]. Recently, Kaniadakis statistics have been utilized as a generalized measure of entropy [43]- [45] to investigate various gravitational and cosmological phenomena. Kaniadakis entropy modifies the standard thermodynamics, allowing for non-linearities that account for a broader range of behaviors in dark energy. It provides a more generalized equation of state, enabling flexibility in describing the evolution of dark energy over cosmic time. The generalized $\mathcal{K}$-entropy, or Kaniadakis entropy, which characterizes black hole entropy, can be expressed with a single free parameter [46].

$$S_{\mathcal{K}}=\frac{1}{\mathcal{K}}sinh(\mathcal{K}\,S_{BH}) \tag{1}$$

Cite as: Y. Aditya, D. Tejeswararao, U.Y.D. Prasanthi, D. Ram Babu, East Eur. J. Phys. 1, 9 (2025), https://doi.org/10.26565/2312-4334-2025-1-01

where $\mathcal{K}$ is an unknown parameter. Thus, by using the concept of entropy and the notion of HDE, a novel model of DE called Kaniadakis HDE (KHDE) is proposed [46], which exhibits significant characteristics. Jawad and Sultan [47], Sharma [48], and Drepanou et al. [49] have examined KHDE models inside various gravitational theories. The dynamic structures of HDE, as investigated by Sadeghi et al. [50], have been analyzed within the context of BD's theory of gravity, using the Tsallis and Kaniadakis approaches. Rao et al. [51] explored KHDE model in GTR. The integration of KHDE within Barber's second self-creation theory of gravitation enhances both the theoretical framework for gravity and DE. It provides a dynamic, thermodynamically consistent solution to cosmological problems such as the cosmological constant and cosmic acceleration. By linking gravity's evolution with a generalized, non-linear description of DE, this combination could offer deeper insights into the structure of the universe and the nature of its expansion.

Several studies provide information about how the large-scale structure we see today might have developed from tiny anisotropies. The conditions of the early universe before it attained the isotropic state can be modeled using Binachi type(BT)-II space-time. For theories explaining how the universe changed from a highly anisotropic state to its current isotropic state, this is essential. Potential anisotropies and abnormalities in the CMB are studied using Bianchi models, such as type-II. These investigations aid in determining the effect of anisotropic expansion on the CMB and evaluating the universe's isotropy. The discussion above makes it evident that a number of authors have looked into KHDE models of the universe. The BT-II KHDE model has not yet been studied in the literature in relation to the self-creation theory of gravity. In this work, we consider the self-creation theory of gravity in the setting of the BT-II universe, which includes matter and KHDE.

With this motivation, in this work we construct Bianchi type-II KHDE model with Hubble horizon as IR cutoff in self-creation theory of gravitation. The following is how the paper has been arranged: The field equations in self creation theory of gravity pertaining to the KHDE source are formulated along with their solution in section-2. Section-3 provides cosmological parameters and their physical discussion. Final remarks are presented in section-4.

2. FIELD EQUATIONS AND MODEL

We consider BT-II metric of the form

$$ds^2 = -dt^2 + R(t)^2dx^2 + S(t)^2dy^2 + 2S(t)^2xdydz + (S(t)^2x^2 + R(t)^2)dz^2. \tag{2}$$

The self-creation theory field equations are as follows:

$$R_{ij} - \frac{1}{2}Rg_{ij} = \frac{-8\pi}{\phi}(T_{ij} + \overline{T}_{ij}), \tag{3}$$

$$\Box\phi = \phi^{;\nu}_{;\nu} = \frac{8\pi\mu}{3}(T + \overline{T}). \tag{4}$$

In this context, the symbols have their usual meaning. The stress-energy tensors for matter distribution is as follows.

$$T_{ij} = diag[0, 0, 0, -1]\rho_m, \quad \overline{T}_{ij} = diag[\omega_{de}, \omega_{de} + \gamma, \omega_{de}, -1]\rho_{de}. \tag{5}$$

The field equations for the space-time (2), using the comoving coordinate system and the above equations (3) and (4), may be represented as:

$$\frac{\ddot{S}}{S} + \frac{\ddot{R}}{R} + \frac{\dot{R}}{R}\frac{\dot{S}}{S} + \frac{S^2}{4R^4} = \frac{-8\pi\omega_{de}\rho_{de}}{\phi} \tag{6}$$

$$\frac{\dot{R}^2}{R^2} + \frac{2\ddot{R}}{R} - \frac{3S^2}{4R^4} = \frac{-8\pi(\omega_{de} + \gamma)\rho_{de}}{\phi} \tag{7}$$

$$\frac{\ddot{R}}{R} + \frac{\ddot{S}}{S} + \frac{\dot{S}}{S}\frac{\dot{R}}{R} + \frac{S^2}{4R^4} = -8\pi\omega_{de}\rho_{de} \tag{8}$$

$$\frac{2\dot{R}\dot{S}}{RS} + \frac{\dot{R}^2}{R^2} - \frac{S^2}{4R^4} = \frac{8\pi[\rho_m + \rho_{de}]}{\phi} \tag{9}$$

$$\dot{\phi}\left(\frac{\dot{S}}{S} + \frac{2\dot{R}}{R}\right) + \ddot{\phi} = \frac{8\pi\mu(T + \overline{T})}{3}. \tag{10}$$

Differentiation with respect to time t is represented by a dot above a variable in this notation. We can solve this system appropriately with the use of assumptions which connects unknowns in the field equations. Because of this, we take into account the following physically plausible circumstances:

$$R = S^k \tag{11}$$

Here, k denotes a constant (Collins et al. [55]). Observations of velocity-redshift from extragalactic sources indicate that the Hubble expansion of the present universe is isotropic to within 30% [52]-[54]. Additionally, redshift surveys place a constraint on $\frac{\sigma}{H} \leq 0.3$ within our current Galaxy.

Additionally, it is common in the literature to assume a power-law relationship between ϕ and the average scale factor $a(t)$, expressed as [56, 57]: $\phi \propto [a(t)]^n$, where n is the power index. Various researchers have explored different properties of scalar fields following this relationship. Considering the physical relevance of this relationship, we adopt following assumption

$$\phi(t) = \phi_0[a(t)]^n. \tag{12}$$

Using the relations (11) and (12) in Eqs. (6) and (7), we obtain the metric potentials as

$$R = (b_3 e^{\gamma_0 t} + b_4)^{\frac{1}{k+2}} \tag{13}$$

and

$$S = (b_3 e^{\gamma_0 t} + b_4)^{\frac{k}{k+2}} \tag{14}$$

where $b_3 = \frac{(k+2)b_1}{\gamma_0}$, $b_4 = (k+2)b_2$, b_1 and b_2 are integrating constants. The scalar field of the model is

$$\phi = \phi_0 \left(b_3 e^{\gamma_0 t} + b_4\right)^{\frac{n}{3}}. \tag{15}$$

Now metric (2), with the aid of Eqs. (13) and (14), can be written as

$$\begin{aligned} ds^2 = -dt^2 + (b_3 e^{\gamma_0 t} + b_4)^{\frac{2}{k+2}} dx^2 + (b_3 e^{\gamma_0 t} + b_4)^{\frac{2k}{k+2}} dy^2 + 2(b_3 e^{\gamma_0 t} + b_4)^{\frac{2k}{k+2}} x dy dz \\ +((b_3 e^{\gamma_0 t} + b_4)^{\frac{2k}{k+2}} x^2 + (b_3 e^{\gamma_0 t} + b_4)^{\frac{2}{k+2}}) dz^2. \end{aligned} \tag{16}$$

Equation (16) describes a anisotropic BT-II KHDE model within the context of self-creation gravity theory, with the following physical parameters. The model's average scale factor $a(t)$ and volume $V(t)$ are defined as follows:

$$V(t) = a(t)^3 = (b_3 e^{\gamma_0 t} + b_4). \tag{17}$$

The expressions for the mean Hubble H and the expansion scalar θ parameters are derived as follows:

$$H = 3\theta = \frac{b_3 \gamma_0 e^{\gamma_0 t}}{3\, b_3 e^{\gamma_0 t} + 3\, b_4}. \tag{18}$$

The average anisotropic parameter A_h and shear scalar σ^2 are given by

$$\sigma^2 = \frac{(k-1)^2 b_3^2 \gamma_0^2 e^{2\gamma_0 t}}{(k+2)^2 \left(b_3 e^{\gamma_0 t} + b_4\right)^2} \; ; \; A_h = \frac{2(k-1)^2}{(k+2)^2}. \tag{19}$$

From the aforementioned parameters, it is evident that both the spatial volume of the universe demonstrate its exponential expansion. Moreover, during the initial epoch, all values become finite. However, as t tends to infinity, they diverge. Notably, when $k = 1$, the model achieves shear-free and isotropic characteristics, as indicated by the conditions $\sigma^2 = 0$ and $A_h = 0$.

According to the HDE theory, for DE is responsible for the accelerated expansion, the total vacuum energy contained within a region of size $\mathcal{L}$ must be less than or equal to the energy of a black hole of the same size, as governed by the Kaniadakis black hole entropy equation (Eq. (1)). This leads to the following condition:

$$\Lambda^4 \equiv \rho_{de} \propto \frac{S_{\mathcal{K}}}{\mathcal{L}^4} \tag{20}$$

for the energy density ρ_{de}. Now, IR cutoff is taken as Hubble horizon (i.e., $\mathcal{L} = \frac{1}{H}$; $A = \frac{4\pi}{H^2}$),

$$\rho_{de} = \frac{3c^2 H^4}{\mathcal{K}} sinh\left(\frac{\pi\mathcal{K}}{H^2}\right) \tag{21}$$

in this formulation, the constant c^2 remains unknown, $\mathcal{K}$ is a real-valued parameter, and the Hubble parameter is given by $H = \frac{\dot{a}}{a}$. It follows that, as $k \longrightarrow 0$, we retrieve the well-established Bekenstein entropy-based HDE expression, $\rho_{de} \rightarrow \frac{3c^2H^4}{\mathcal{K}}$. In addition, we account for a pressureless fluid with energy density ρ_m and a DE component with pressure p_{de} and density ρ_{de}.

Using $H(t)$ in the above Eq. (21), we get the energy density of KHDE of the model as

$$\rho_{de} = \frac{3c^2{b_3}^4{\gamma_0}^4\left(e^{\gamma_0 t}\right)^4}{\left(3\,b_3e^{\gamma_0 t}+3\,b_4\right)^4\mathcal{K}}\sinh\left(\frac{\pi\,\mathcal{K}\,\left(3\,b_3e^{\gamma_0 t}+3\,b_4\right)^2}{{b_3}^2{\gamma_0}^2\left(e^{\gamma_0 t}\right)^2}\right). \tag{22}$$

Using Eqs. (13)-(15) and (22) in Eq. (9), we get the energy density of matter as

$$\begin{aligned}\rho_m \quad = \quad & \frac{\phi_0\left(b_3e^{\gamma_0 t}+b_4\right)^{n/3}}{8\pi}\left[\frac{{b_3}^2{\gamma_0}^2\left(e^{\gamma_0 t}\right)^2}{(k+2)^2\left(b_3e^{\gamma_0 t}+b_4\right)^2}+\frac{2{b_3}^2{\gamma_0}^2\left(e^{\gamma_0 t}\right)^2k}{(k+2)^2\left(b_3e^{\gamma_0 t}+b_4\right)^2}\right.\\ & \left.-\frac{\left(b_3e^{\gamma_0 t}+b_4\right)^{\frac{2k}{k+2}}}{4\left(b_3e^{\gamma_0 t}+b_4\right)^{\frac{4}{k+2}}}\right]-\frac{3c^2{b_3}^4{\gamma_0}^4\left(e^{\gamma_0 t}\right)^4}{\left(3\,b_3e^{\gamma_0 t}+3\,b_4\right)^4\mathcal{K}}\sinh\left(\frac{\pi\,\mathcal{K}\,\left(3\,b_3e^{\gamma_0 t}+3\,b_4\right)^2}{{b_3}^2{\gamma_0}^2\left(e^{\gamma_0 t}\right)^2}\right).\end{aligned} \tag{23}$$

Using Eqs. (13)-(15), (21) in Eq. (6), we obtain the EoS parameter of KHDE as

$$\begin{aligned}\omega_{de} \quad = \quad & -\frac{\phi_0\left(b_3e^{\gamma_0 t}+b_4\right)^{n/3}\left(3\,b_3e^{\gamma_0 t}+3\,b_4\right)^4\mathcal{K}}{24\pi\,c^2{b_3}^4{\gamma_0}^4\left(e^{\gamma_0 t}\right)^4}\left(\frac{{b_3}^2{\gamma_0}^2\left(e^{\gamma_0 t}\right)^2+(k+2)\,b_3b_4{\gamma_0}^2e^{\gamma_0 t}}{(k+2)^2\left(b_3e^{\gamma_0 t}+b_4\right)^2}\right.\\ & +\frac{k^2{b_3}^2{\gamma_0}^2\left(e^{\gamma_0 t}\right)^2+k\,(k+2)\,b_3b_4{\gamma_0}^2e^{\gamma_0 t}}{(k+2)^2\left(b_3e^{\gamma_0 t}+b_4\right)^2}+\frac{{b_3}^2{\gamma_0}^2\left(e^{\gamma_0 t}\right)^2k}{(k+2)^2\left(b_3e^{\gamma_0 t}+b_4\right)^2}\\ & \left.+\frac{1}{4\left(\left(b_3e^{\gamma_0 t}+b_4\right)^{4(k+2)^{-1}}\right)}\left(b_3e^{\gamma_0 t}+b_4\right)^{\frac{k}{k+2}}\right)\left(\sinh\left(\frac{\pi\,\mathcal{K}\,\left(3\,b_3e^{\gamma_0 t}+3\,b_4\right)^2}{{b_3}^2{\gamma_0}^2\left(e^{\gamma_0 t}\right)^2}\right)\right)^{-1}.\end{aligned} \tag{24}$$

The skewness parameter is determined as

$$\begin{aligned}\gamma \quad = \quad & \frac{\phi_0\left(b_3e^{\gamma_0 t}+b_4\right)^{n/3}\left(3\,b_3e^{\gamma_0 t}+3\,b_4\right)^4\mathcal{K}}{24\pi\,c^2{b_3}^4{\gamma_0}^4\left(e^{\gamma_0 t}\right)^4}\left(\left(b_3e^{\gamma_0 t}+b_4\right)^{\frac{2k-4}{k+2}}-\frac{{\gamma_0}^2\,(1-k)\,b_3e^{\gamma_0 t}}{(k+2)\left(b_3e^{\gamma_0 t}+b_4\right)}\right)\\ & \times\left(\sinh\left(\frac{\pi\,\mathcal{K}\,\left(3\,b_3e^{\gamma_0 t}+3\,b_4\right)^2}{{b_3}^2{\gamma_0}^2\left(e^{\gamma_0 t}\right)^2}\right)\right)^{-1}.\end{aligned} \tag{25}$$

3. COSMOLOGICAL PARAMETERS AND PHYSICAL DISCUSSION

In this section, we investigate the expansion of the universe by scrutinizing various cosmological parameters. These parameters include the energy conditions, the scalar field ($\phi(t)$), the EoS (ω_{de}), the squared sound speed (v_s^2), the deceleration (q) parameters, as well as cosmic planes like $\omega_{de} - \omega'_{de}$ and statefinder planes for the anisotropic KHDE model.

Scalar field: Fig. 1 illustrates the evolution of the scalar field with time. The scalar field maintains a positive value and demonstrates a consistent decrease over time. This declining trend of the scalar field suggests a concurrent increase in kinetic energy within the model. Additionally, it has been observed that as the parameter k rises, the scalar field exhibits a decreasing behavior.

EoS parameter (ω): It serves as a crucial tool for categorizing the various phases in the expanding universe. It is expressed as $\omega = \frac{p}{\rho}$, representing the relationship between pressure (p) and energy density (ρ) within a given matter distribution. Different phases, characterized by deceleration or acceleration, correspond to specific ranges of ω:

Deceleration phases encompass intervals such as those involving cold dark matter or dust fluid (ω equals zero), indicating the radiation era when ω lies between 0 and $1/3$, and the fluid is classified as stiff for $\omega = 1$. The accelerating phase, akin to the cosmic constant/vacuum period (ω equals -1), corresponds to the quintessence period when $-1 < \omega < -1/3$, and it's known as the phantom era when $\omega < -1$. This signifies a quintom period characterized by a combination of both quintessence and phantom components.

The EoS parameter of KHDE with the Hubble horizon cutoff is provided in Eq. (24). Fig. 2 illustrates the evolution of the EoS parameter ω_{de} concerning cosmic time t. Initially, as depicted in Fig. 2, ω_{de} originates from the DE era, transitioning through the aggressive phantom region ($\omega_{de} << -1$) and into the phantom region ($\omega_{de} < -1$) and quintessence as well as ΛCDM model for three values of c respectively. With decreasing values of the parameter c, our model is progressively enters the quintessence region.

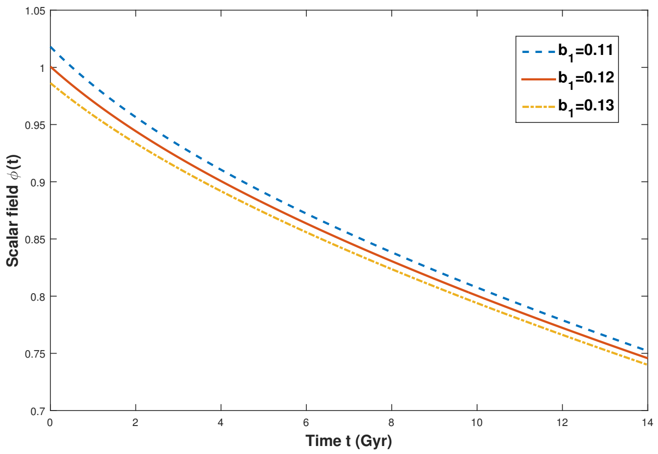

Figure 1. Scalar field Vs. t for $\gamma_0 = 0.178$, $k = 0.97$, $n = -0.28$, $b_2 = -0.34$ and $\phi_0 = 1$.

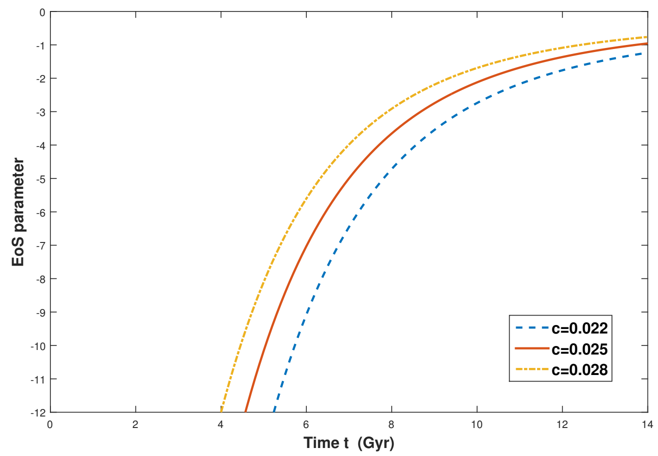

Figure 2. EoS parameter Vs. t for $\gamma_0 = 0.178$, $k = 0.97$, $n = -0.28$, $b_2 = -0.34$, $\phi_0 = 1$, $b_1 = 0.12$ and $\mathcal{K} = 0.007$.

Squared sound speed: It is derived as

$$v_s^2 = \frac{\dot{p}_{de}}{\dot{\rho}_{de}} = \omega_{de} + \frac{\rho_{de}}{\dot{\rho}_{de}}\,\dot{\omega}_{de}. \tag{26}$$

The sign of v_s^2 is crucial in assessing the stability of DE models. A positive signature of v_s^2 indicates model stability, while a negative signature suggests instability. By substituting the energy density and EoS parameter from equations (22) and (24) into the equation for squared sound speed (v_s^2) provided by equation (26), we conduct a graphical analysis of v_s^2 for our model. As illustrated in Fig. 3, the trajectories are negative at initial epoch and consistently exhibit positive behavior at later stages of the evolution of the model. Consequently, this indicates that our model is unstable at initial epoch whereas it becomes stable at present and late-times.

ω_{de}–ω'_{de} **plane:** We examine the $\omega_{de} - \omega'_{de}$ plane, where ω'_{de} represents the rate of change of the EoS parameter ω_{de} with respect to $\ln(a(t))$ [58]. It has also been found that the $\omega_{de} - \omega'_{de}$ plane can be split into two regions: thawing ($\omega_{de} < 0$, $\omega'_{de} > 0$) and freezing ($\omega_{de} < 0$, $\omega'_{de} < 0$). The freezing region corresponds to a phase of faster cosmic acceleration compared to the thawing region.

Fig. 4 illustrates the relationship between the $\omega_{de} - \omega'_{de}$ plane and different values of c. It shows that the $\omega_{de} - \omega'_{de}$ plane predominantly corresponds to the thawing region, irrespective of the specific parameter values. Moreover, the current values of ω_{de} and ω'_{de} align well with present observational data.

Energy conditions: The Raychaudhuri equations initiated the exploration of energy conditions, playing a crucial role in analyzing the alignment of null and time-like geodesics. The energy conditions are used to illustrate other universal

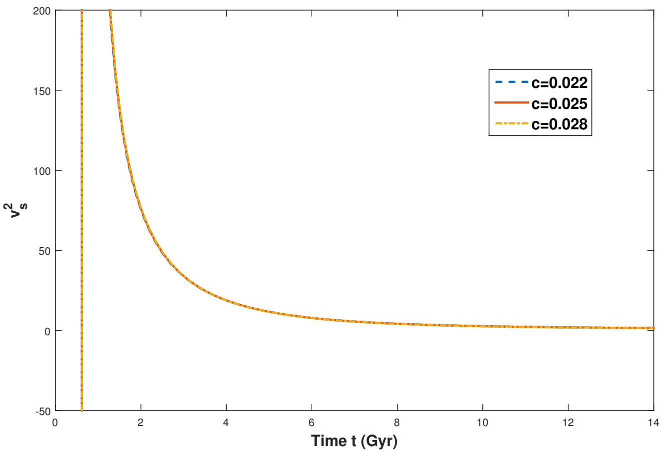

Figure 3. v_s^2 Vs. t for $\gamma_0 = 0.178$, $k = 0.97$, $n = -0.28$, $b_2 = -0.34$, $\phi_0 = 1$, $b_1 = 0.12$ and $\mathcal{K} = 0.007$.

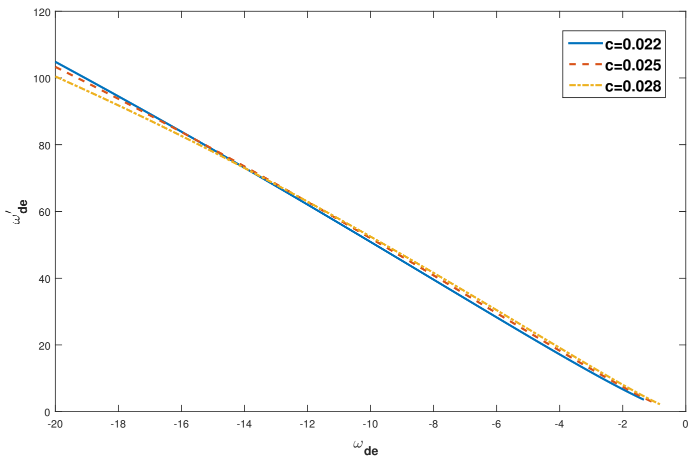

Figure 4. ω_{de}–ω'_{de} plane for $\gamma_0 = 0.178$, $k = 0.97$, $b_1 = 0.12$, $n = -0.28$, $b_2 = -0.34$, $\phi_0 = 1$ and $\mathcal{K} = 0.007$.

principles about the dynamics of intense gravitational fields. The often observed energy conditions are as follows:

Dominant energy condition (DEC): $\rho_{de} \geq 0$, $\rho_{de} \pm p_{de} \geq 0$.

Strong energy conditions (SEC) : $\rho_{de} + p_{de} \geq 0$, $\rho_{de} + 3p_{de} \geq 0$,

Null energy conditions (NEC): $\rho_{de} + p_{de} \geq 0$,

Weak energy conditions (WEC): $\rho_{de} \geq 0$, $\rho_{de} + p_{de} \geq 0$,

Fig. 5 illustrates the energy conditions of our KHDE model. It is evident that the WEC is satisfied, as $\rho_{de} \geq 0$. However, the SEC $\rho_{de} + 3p_{de} \geq 0$ is not met. This observation, reflecting the universe's acceleration in its later stages, is consistent with contemporary observational evidence.

Deceleration parameter: The expansion of the universe is often described using deceleration parameter (DP). Positive values of the DP indicate that the model exhibits a decelerating expansion in the usual sense. When $q = 0$, the universe expands at a constant rate. Accelerated expansion takes place when q lies between -1 and 0, while super-exponential expansion occurs when q is less than -1. The DP can be calculated as follows:

$$q = -1 + \frac{d}{dt}\left(\frac{1}{H(t)}\right) = -1 - \frac{3b_4}{b_3 e^{\gamma_0 t}}. \tag{27}$$

Fig. 6 depicts the evolution of the DP q as a function of time t. Notably, our model shows a transition from the early decelerating phase to the current accelerating era, in agreement with recent observational data. Furthermore, the current value of the DP ($q_0 \approx -0.86$) closely matches contemporary observational results.

Statefinder parameters: Various DE models have emerged in recent years, aiming to elucidate the accelerating expansion of the universe. Interestingly, these models often yield identical values for the current Hubble and deceleration

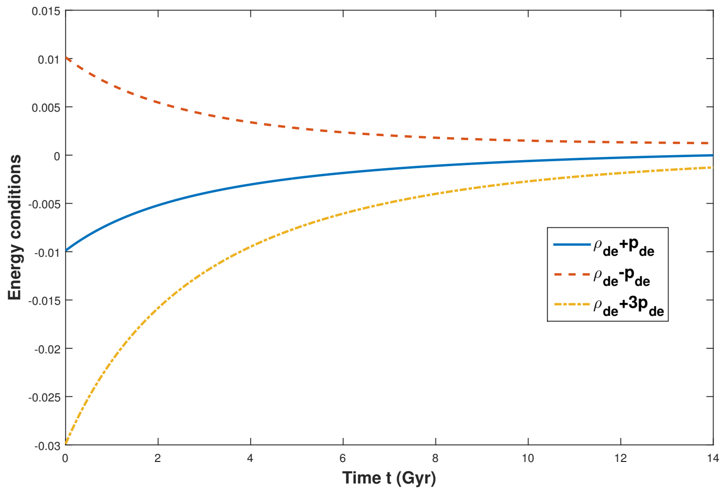

Figure 5. Energy conditions Vs. t for $\gamma_0 = 0.178$, $k = 0.97$, $n = -0.28$, $b_1 = 0.12$, $c = 0.025$, $b_2 = -0.34$, $\phi_0 = 1$, $c = 0.028$ and $\mathcal{K} = 0.007$.

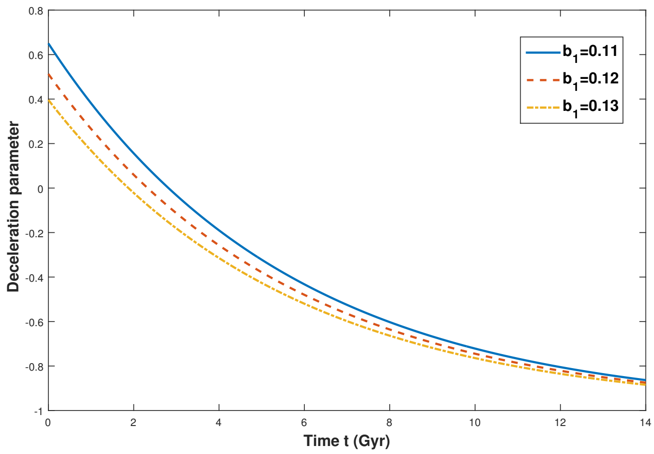

Figure 6. q Vs. t for $\gamma_0 = 0.178$, $k = 0.97$, $n = -0.28$ and $b_2 = -0.34$.

parameters, making them practically indistinguishable from one another. Sahni et al. [59] proposed a merger of the deceleration and Hubble parameters, expressed as:

$$r = \frac{\dddot{a}}{aH^3}, \quad s = \frac{r-1}{3(q-1/2)}. \tag{28}$$

The statefinder parameters for our model are

$$r = 1 + \frac{9{b_4}^2}{{b_3}^2\left(e^{\gamma_0 t}\right)^2} \tag{29}$$

$$s = \frac{{b_4}^2}{{b_3}^2\left(e^{\gamma_0 t}\right)^2}\left(-\frac{1}{2} - \frac{b_4}{b_3 e^{\gamma_0 t}}\right)^{-1} \tag{30}$$

The regions shown below are defined by these statefinders: ΛCDM for $(r,s) = (1,0)$ and CDM model for $(r,s) = (1,1)$; $r< 1$ gives quintessence and $s> 0$ gives phantom DE phases; $r> 1$ with $s< 0$ establishes the Chaplygin gas model. Fig. 7 depicts the $r-s$ plane's trajectory. The $r-s$ plane resembles to the quintessence as well as phantom regions it its evolution.

Comparative analysis: Here, we compare our work with recent studies on this subject and discuss its alignment with observational data.

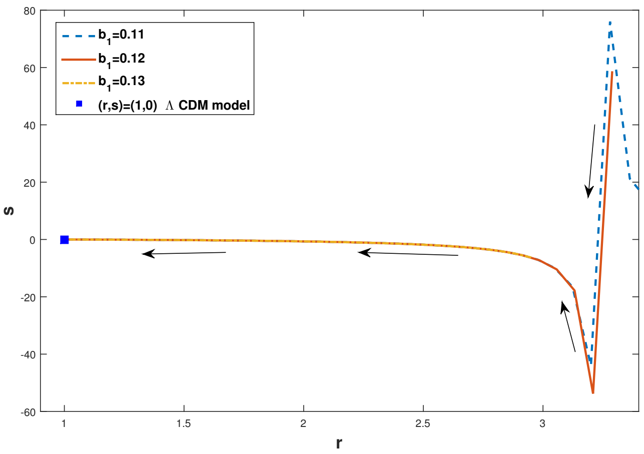

Figure 7. Statefinder parameters for $\gamma_0 = 0.178$, $k = 0.97$, $n = -0.28$, $b_1 = 0.12$ and $b_2 = -0.34$.

Rao and Prasanthi [60] conducted an investigation into BT-I and BT-III DE models within the framework of SB theory. These models evolve from the phantom region and gradually transition into the quintessence region. Similarly, Rao et al. [39] examined a universe filled with holographic Ricci DE. Their model sees the EoS parameter evolve from a matter-dominated state to the phantom region, crossing the phantom divide line and ultimately progressing towards the quintessence region as time advances. Sadri and Vakili [61] explored the FRW new HDE model within the BD gravity. Their findings revealed that the EoS parameter could enter the phantom era without requiring any interaction between DE and dark matter. Aditya and Reddy [62] studied BT-I universe within the SB scalar–tensor theory and it begins in the matter-dominated era, progresses through the quintessence region, crosses the phantom divide line, and ultimately stabilizes in the phantom region. Prasanthi and Aditya [63] delved into BT-VI$_0$ RHDE models in GTR, where they observed the universe exhibiting both quintom and phantom behaviors. Naidu et al. [64] analyzed the FRW-type DE cosmological models within the SB gravity. Aditya [65] examined the BT-I RHDE model in SB theory and determined that it demonstrated quintom behavior while aligning with observational data. Aditya and Prasanthi [66] looked into the dynamics of SMHDE in the BD gravity, finding that their model starts in the matter-dominated era, crosses the phantom divide line, and ultimately stabilizes in the aggressive phantom region. Dasunaidu et al. [67] explored FRW-type DE models in SB's theory, observing that the models evolve from the matter-dominated era, pass through the quintessence DE phase, and finally approach vacuum DE and the phantom era. Rao et al. [51] studied the BT-VI$_0$ KHDE model in GTR, asserting that the model starts in the matter-dominated era, evolves through the quintessence region, and eventually becomes the ΛCDM model. Aditya et al. [68] explored BT-VI$_0$ space-time within the SMHDE framework in the BD theory of gravitation, concluding that the model accurately characterizes both the quintessence and vacuum regions of the universe. Prasanthi et al. [69] investigated the KHDE model within the BD gravity, particularly in the Kantowski-Sachs space-time. Murali et al. [70] explored the BT-I universe KHDE model within SB theory, claiming that these models closely resemble the ΛCDM limit at late times and match recent observational data. In comparison to these studies, our models align with existing results in the literature. The analysis of the EoS parameter shows that our model begins in the aggressive phantom region ($\omega_{de} \ll -1$) and eventually transitions into the ΛCDM model ($\omega_{de} = -1$), exhibiting behavior that closely mirrors the models discussed above. Furthermore, the observational data from the Planck mission, as presented by Aghanim et al. [71], provide constraints on the EoS parameter of DE, with the following ranges: $\omega_{de} = -1.56^{+0.60}_{-0.48}$ (Planck + TT + lowE); $\omega_{de} = -1.58^{+0.52}_{-0.41}$ (Planck + TT, TE, EE + lowE); $\omega_{de} = -1.57^{+0.50}_{-0.40}$ (Planck + TT, TE, EE + lowE + lensing); and $\omega_{de} = -1.04^{+0.10}_{-0.10}$ (Planck + TT, TE, EE + lowE + lensing + BAO) at a 95% confidence level. As shown in Fig. 2, the EoS parameter of our model lies comfortably within these observational limits, further reinforcing the consistency of our results with cosmological data.

Moreover, the trajectories of the $\omega_{de} - \omega'_{de}$ plane derived from our model intersect with the observational data reported by various studies [73, 74]. Specifically, the values of ω_{de} and ω'_{de} obtained from our model fall within the ranges provided by observations from the Planck mission: $\omega_{de} = -1.13^{+0.24}_{-0.25}$, $\omega'_{de} < 1.32$ (Planck + WP + BAO); and $\omega_{de} = -1.34 \pm 0.18$, $\omega'_{de} = 0.85 \pm 0.7$ (WMAP + eCAMB + BAO + H_0). This alignment further affirms the credibility of our model's predictions and its consistency with observational data. Finally, the current values of the deceleration parameter q from our model align well with those derived from observational data—$q = -0.930 \pm 0.218$ (BAO + Masers + TDSL + Pantheon + H_z) and $q = -1.2037 \pm 0.175$ (BAO + Masers + TDSL + Pantheon + H_0 + H_z) as reported by Capozziello et al. [72]. This alignment underscores the reliability and accuracy of our model's predictions, indicating that our KHDE model is more viable than the DE models proposed by several other authors.

4. CONCLUSIONS

A cosmological reconstruction of the second self-creation gravity has been studied in this study using the KHDE model. Both the geometric and matter components are considered to have contributed to the acceleration of the expansion of the Universe. The BT-II Universe with a pressure-less matter contribution as cosmic fluid configuration has been studied and the associated field equations have been derived. Using energy conditions, deceleration parameters, and the EoS, the reconstruction of the KHDE model has been examined for its evolutionary behavior. We also investigated the (r, s) and $\omega_{de} - \omega'_{de}$ cosmic planes to learn more about how the model changed over time. Here are the main takeaways from our research.

i. According to Fig. 2 (the EoS parameter trajectory), the model begins in the aggressive phantom region and eventually approaches the ΛCDM model and the phantom phase of the Universe.

ii. The model smoothly moves from the early decelerated epoch to the present accelerated era of the Universe when the DP evolves against cosmic time (Fig. 6). According to Fig. 7, the statefinder diagnostic plane of our rebuilt model aligns with both the phantom and Chaplygin gas models.

iii. The thawing region is depicted by the track in the $\omega_{de} - \omega'_{de}$ plane (Fig. 4). According to Fig. 3, our model is unstable at the first period but becomes stable over the present and late times. The energy conditions shown in Fig. 5 are from our KHDE model. While the SEC has not been satisfied, the WEC has been satisfied. Therefore, according to modern observational evidence (Fig. 5), the cosmos is expanding at an accelerated rate in its latter phases.

Acknowledgment: Y. Aditya expresses gratitude to the National Board for Higher Mathematics, Department of Atomic Energy, Government of India, for their financial support under grant No: 02011/8/2023 NBHM(R.P.)/R & D II/3073.

ORCID

Y. Aditya, https://orcid.org/0000-0002-5468-9697; **D. Tejeswararao**, https://orcid.org/0000-0003-3508-346X; **U.Y. Divya Prasanthi**, https://orcid.org/0009-0004-5397-050X; **D. Ram Babu**, https://orcid.org/0009-0008-7791-5977

REFERENCES

[1] S. Perlmutter, et al., Astrophys. J. **517**, 565 (1999). https://doi.org/10.1086/307221

[2] A. G. Riess, et al., Astron. Soc. Pac. **112**, 1284 (2000). https://doi.org/10.1086/316624

[3] M. Tegmark, et al., Phys. Rev. D, **69**, 103501 (2004). https://doi.org/10.1103/PhysRevD.69.103501

[4] M. Sharif, and Z.J. Yousaf, Astropart. Phys. **56**, 19 (2014). https://doi.org/10.1016/j.astropartphys.2014.02.006

[5] S. Nojiri, and S. Odintsov, Phys. Lett. B. **631**, 1 (2005). https://doi.org/10.1016/j.physletb.2005.10.010

[6] T. Harko, and F.S.N. Lobo, Int. J. Mod. Phys. D, **21**, 1242019 (2012). https://doi.org/10.1142/S0218271812420199

[7] C. Brans, and R.H., Dicke, Phys. Rev. **124**, 925 (1961). https://doi.org/10.1103/PhysRev.124.925

[8] D. Saez, and V.J. Ballester, Phys. Lett. A, **113**, 467 (1986). https://doi.org/10.1016/0375-9601(86)90121-0

[9] G.A. Barber, Gen. Relativ. Gravit. **14**, 117 (1982). https://doi.org/10.1007/BF00756918

[10] T. Singh, and T. Singh, Astrophys. Space Sci. **102**, 67 (1984). https://doi.org/10.1007/BF00651062

[11] D.R.K. Reddy, Astrophys. Space Sci. **133**, 389 (1987). https://doi.org/10.1007/BF00642496

[12] V.U.M. Rao, et al., Astrophys Space Sci. **317**, 83 (2008). https://doi.org/10.1007/s10509-008-9859-7

[13] R.L. Naidu, et al.: Astrophys Space Sci. **358**, 23 (2015). https://doi.org/10.1007/s10509-015-2421-5

[14] V.U.M. Rao, and U.Y.D. Prasanthi, Can. J. Phys. **95(6)**, 554 (2017). https://doi.org/10.1139/cjp-2017-0014

[15] R.R. Caldwell, and M. Kamionkowski, Ann. Rev. Nucl. Part. Sci. **59**, 397 (2009). https://doi.org/10.1146/annurev-nucl-010709-151330

[16] K. Bamba, et al., Astrophys. Space Sci. **342**, 155 (2012). https://doi.org/10.1007/s10509-012-1181-8

[17] S. Nojiri, et al., Phys. Rept. **692**, 1 (2017). https://doi.org/10.1016/j.physrep.2017.06.001

[18] Y. Aditya, and D.R.K. Reddy, Eur. Phys. J. C, **78**, 619 (2018). https://doi.org/10.1140/epjc/s10052-018-6074-8

[19] V.U.M. Rao, et al., Results in Physics, **10**, 469 (2018). https://doi.org/10.1016/j.rinp.2018.06.027

[20] Y. Aditya, et al., Eur. Phys. J. C, **79**, 1020 (2019). https://doi.org/10.1140/epjc/s10052-019-7534-5

[21] U.K. Sharma, et al., IJMPD, **31**, 2250013 (2022). https://doi.org/10.1142/S0218271822500134

[22] U.Y.D. Prasanthi, and Y. Aditya, Results of Physics **17**, 103101 (2020). https://doi.org/10.1016/j.rinp.2020.103101

[23] U.Y.D. Prasanthi, and Y. Aditya, Physics of the dark universe **31**, 100782 (2021). https://doi.org/10.1016/j.dark.2021.100782

[24] Y. Aditya, and D.R.K. Reddy, Astrophys. Space Sci. **363**, 207 (2018). https://doi.org/10.1007/s10509-018-3429-4

[25] Y Aditya, et al., Results in Physics, **12**, 339 (2019). https://doi.org/10.1016/j.rinp.2018.11.074

[26] Y. Aditya, et al. Astrophys. Space Sci. **364**, 190 (2019). https://doi.org/10.1007/s10509-019-3681-2

[27] Y. Aditya, et al., Int. J. Mod. Phys. A, **37**, 2250107 (2022). https://doi.org/10.1142/S0217751X2250107X
[28] A. Jawad, et al., Symmetry, **10**, 635 (2018). https://doi.org/10.3390/sym10110635
[29] A. Riess, et al., Astron. J. **116**, 1009 (1998). https://doi.org/10.1086/300499
[30] B. Jain, and A. Taylor, Phys. Rev. Lett. **91**, 141302 (2003). https://doi.org/10.1103/PhysRevLett.91.141302
[31] L. Susskind, J. Math. Phys. **36**, 6377 (1994). https://doi.org/10.1063/1.531249
[32] R. Bousso, JHEP, **07**, 004 (1999). https://doi.org/10.1088/1126-6708/1999/07/004
[33] A. Cohen, et al.: Phys. Rev. Lett. **82**, 4971 (1999). https://doi.org/10.1103/PhysRevLett.82.4971
[34] M. Tavayef, et al., Phys. Lett. B, **781**, 195 (2018). https://doi.org/10.1016/j.physletb.2018.04.001
[35] C. Tsallis, and L.J.L. Cirto, Eur. Phys. J. C, **73**, 2487 (2013). https://doi.org/10.1140/epjc/s10052-013-2487-6
[36] A.S. Jahromi, et al., Phys. Lett. B, **780**, 21 (2018). https://doi.org/10.1016/j.physletb.2018.02.052
[37] H. Moradpour, et al., Eur. Phys. J. C, **78**, 829 (2018). https://doi.org/10.1140/epjc/s10052-018-6309-8
[38] Y. Aditya, and D.R.K. Reddy, Eur. Phys. J. C, **78**, 619 (2018). https://doi.org/10.1140/epjc/s10052-018-6074-8
[39] V.U.M. Rao, et al., Results in Physics, **10**, 469 (2018). https://doi.org/10.1016/j.rinp.2018.06.027
[40] M.V. Santhi, et al., Int. J. Theor. Phys. **56**, 362 (2017). https://doi.org/10.1007/s10773-016-3175-8
[41] Y. Aditya, et al., Eur. Phys. J. C, **79**, 1020 (2019). https://doi.org/10.1140/epjc/s10052-019-7534-5
[42] A. Iqbal, A. Jawad, Physics of the Dark Universe, **26**, 100349 (2019). https://doi.org/10.1016/j.dark.2019.100349
[43] G. Kaniadakis, Physica A: Stat. Mech. and its Appl. **296**(3-4), 405 (2001). https://doi.org/10.1016/S0378-4371(01)00184-4
[44] M. Masi, Phys. Lett. A, **338**, 217 (2005). https://doi.org/10.1016/j.physleta.2005.01.094
[45] E.M. Abreu, et al., EPL (Europhysics Letters), **124**, 30003 (2018). https://doi.org/10.1209/0295-5075/124/30003
[46] H. Moradpour, et al. Eur. Phys. J. C, **80**, 1 (2020). https://doi.org/10.1140/epjc/s10052-020-8307-x
[47] A. Jawad, and A.M. Sultan, Adv. High Energy Phys. **2021**, 5519028 (2021). https://doi.org/10.1155/2021/5519028
[48] U.K. Sharma, et al., IJMPD, **31**, 2250013 (2022). https://doi.org/10.1142/S0218271822500134
[49] N. Drepanou, et al., Eur. Phys. J. C, **82**, 449 (2022). https://doi.org/10.1140/epjc/s10052-022-10415-9
[50] J. Sadeghi, et al., arXiv:2203.04375 (2022). https://doi.org/10.48550/arXiv.2203.04375
[51] B.G. Rao, et al., East Eur. J. Phys. (1), 43 (2024). https://doi.org/10.26565/2312-4334-2024-1-03
[52] K.S. Thorne, Astrophys. J. **148**, 51 (1967). http://dx.doi.org/10.1086/149127
[53] R. Kantowski, and R.K. Sachs, J. Math. Phys. **7**, 433 (1966). https://doi.org/10.1063/1.1704952
[54] J. Kristian, and R.K. Sachs, Astrophys. J. **143**, 379 (1966). https://doi.org/10.1086/148522
[55] C.B. Collins, et al., Gen. Relativ. Gravit. **12**, 805 (1980). https://doi.org/10.1007/BF00763057
[56] V.B. Johri, and R. Sudharsan, Australian Journal of Physics **42(2)**, 215 (1989). https://doi.org/10.1071/PH890215
[57] V.B. Johri, and K. Desikan, Gen Relat Gravit **26**, 1217 (1994). https://doi.org/10.1007/BF02106714
[58] R. Caldwell, and E.V. Linder, Phys. Rev. Lett. **95**, 141301 (2005). https://doi.org/10.1103/PhysRevLett.95.141301
[59] V. Sahni, et al., J. Exp. Theor. Phys. Lett. **77**, 201 (2003). https://doi.org/10.1134/1.1574831
[60] V.U.M. Rao, and U.Y.D. Prasanthi, The European Physical Journal Plus, **132**, 64 (2017). https://doi.org/10.1140/epjp/i2017-11328-9
[61] E. Sadri, B. Vakili, Astrophysics and Space Science **363**, 13 (2018). https://doi.org/10.1007/s10509-017-3237-2
[62] Y. Aditya, and D.R.K. Reddy, Astrophys. Space Sci. **363**, 207 (2018). https://doi.org/10.1007/s10509-018-3429-4
[63] U.Y. Divya Prasanthi, and Y. Aditya, Results Phys. **17**, 103101 (2020). https://doi.org/10.1016/j.rinp.2020.103101
[64] R.L. Naidu, et al., New Astronomy, **85**, 101564 (2021). https://doi.org/10.1016/j.newast.2020.101564
[65] Y. Aditya, Bulgarian Astronomical Journal **40**, 95 (2024). https://astro.bas.bg/AIJ/issues/n40/YAditya.pdf
[66] Y. Aditya, and U.Y.D. Prasanthi, Bulgarian Astronomical Journal **38**, 52 (2023). https://astro.bas.bg/AIJ/issues/n38/YAditya.pdf
[67] K. Dasunaidu, et al., Bulgarian Astronomical Journal **39**, 72 (2023). https://astro.bas.bg/AIJ/issues/n39/KDasunaidu.pdf
[68] Y. Aditya, et al., East Eur. J. Phys. (1), 85 (2024). https://doi.org/10.26565/2312-4334-2024-1-06
[69] A. V. Prasanthi, et al., East Eur. J. Phys. (2), 10 (2024). https://doi.org/10.26565/2312-4334-2024-2-01
[70] K. Murali, et al., Mod. Phys. Let. A, **39**, 2450106 (2024). https://doi.org/10.1142/S0217732324501062
[71] N. Aghanim, et al., A&A **641**, A6 (2020). https://doi.org/10.1051/0004-6361/201833910
[72] S. Capozziello, et al., MNRAS, **484**, 4484 (2019). https://doi.org/10.1093/mnras/stz176
[73] P.A.R. Ade, et al., Astrophys. **571**, A16 (2014). https://doi.org/10.1051/0004-6361/201321591
[74] G.F. Hinshaw, et al., Astrophys. J. Suppl. **208**, 19 (2018). https://doi.org/10.1088/0067-0049/208/2/19

РЕКОНСТРУКЦІЯ ГОЛОГРАФІЧНОЇ МОДЕЛІ ТЕМНОЇ ЕНЕРГІЇ КАНІАДАКІСА В ТЕОРІЇ САМОСТВОРЕННЯ ГРАВІТАЦІЇ

Ю. Адітья[a], **Д. Техесварарао**[a], **Ю.Й. Дів'я Прасанті**[b], **Д. Рам Бабу**[b]
[a]*Департамент фундаментальних і гуманітарних наук, Технологічний інститут GMR, Раджам-532127, Індія*
[b]*Департамент статистики і математики, Коледж садівництва, Доктор Ю.С.Р. Університет садівництва, Парватіпурам-535502, Індія*

Основною метою цієї статті є дослідження голографічного всесвіту темної енергії Каніадакіса типу Б'янкі II в рамках теорії гравітації самостворення. У цій моделі темної енергії горизонт Хаббла використовується як межа інфрачервоного випромінювання відповідно до голографічної концепції темної енергії Каніадакіса. Ми обчислюємо різні динамічні параметри в цій моделі, включаючи площину вимірювача стану (r, s), параметр сповільнення q, рівняння стану (ω_{de}), квадрат швидкості звуку та площина $\omega_{de} - \omega'_{de}$. Графічний аналіз цих параметрів надається в діапазоні безкоштовних значень параметрів. Результати показують, що параметр уповільнення демонструє плавний перехід Всесвіту від ранньої уповільненої фази до поточного прискореного розширення, тоді як рівняння параметра стану свідчить про фантомну фазу. Площина $\omega_{de} - \omega'_{de}$ досягає області розморожування, а площина вимірювача стану вирівнюється як з фантомною моделлю, так і з газом Чаплигіна. Поточні значення параметрів узгоджуються з наявними даними спостережень, а сильні енергетичні умови виявляються порушеними.

Ключові слова: *Модель Б'янкі типу II; голографічна темна енергія Каніадакіса; теорія самостворення; темна енергія; модифікована теорія гравітації*